

Roles of endoplasmic reticulum stress and autophagy on H₂O₂-induced oxidative stress injury in HepG2 cells

ZHIMING WU¹, HUANGEN WANG¹, SUNYANG FANG¹ and CHAOYANG XU²

¹Department of General Surgery, Shaoxing Hospital, China Medical University;

²Department of Thyroid Breast Surgery, Shaoxing People's Hospital, Shaoxing, Zhejiang 312030, P.R. China

Received March 22, 2017; Accepted March 6, 2018

DOI: 10.3892/mmr.2018.9443

Abstract. Endoplasmic reticulum stress (ERS) can be induced by a variety of physiological and pathological factors including oxidative stress, which triggers the unfolded protein response to deal with ERS. Autophagy has been hypothesized to be a means for tumor cells to increase cell survival under conditions of hypoxia, metabolic stress and even chemotherapy. Although they may function independently from each other, there are also interactions between responses to oxidative stress injury induced by pathologic and pharmacological factors. The aim of the present study was to investigate the effects of ERS and autophagy on H₂O₂-induced oxidative stress injury in human HepG2 hepatoblastoma cells. It was demonstrated that exposure of HepG2 cells to H₂O₂ decreased cell viability and increased reactive oxygen species (ROS) levels in a dosage-dependent manner. In addition, apoptosis and autophagy rates were elevated and reduced following cell exposure to H₂O₂ + the ERS inducer Tunicamycin (TM), and to H₂O₂ + the ERS inhibitor Salubrinal (SAL), compared with the cells treated with H₂O₂ alone, respectively. Further studies revealed that TM enhanced the expression of ERS-related genes including glucose-regulated protein-78/binding immunoglobulin protein, inositol-requiring kinase-I and activating transcription factor 6 and C/EBP-homologous protein 10, which were attenuated by SAL compared with cells exposed to H₂O₂ alone. The data from the present study also demonstrated that LC3II/LC3-I and p62, members of autophagy-related genes, were increased and decreased in cells treated with H₂O₂ + TM compared with cells treated with H₂O₂, respectively, indicating that autophagy was stimulated by ERS. Furthermore, a reduction in the levels of pro caspase-3 and pro caspase-9, and elevation level of caspase-12 were observed in cells exposed to H₂O₂ + TM compared with cells treated

with H₂O₂, respectively, suggesting apoptosis induced by H₂O₂ was enhanced by ERS or autophagy triggered by H₂O₂. The above results suggest that the ERS inducer may be a potential target for pharmacological intervention targeted to ERS or autophagy to enhance oxidative stress injury of tumor cells induced by antitumor drugs.

Introduction

The endoplasmic reticulum (ER) is a common organelle demonstrated in eukaryotic cells, which is an important site for the synthesis and modification of proteins, lipids and carbohydrates (1,2). The ER is also involved in the regulation of the intracellular calcium ion concentration through the storage and release of calcium (3,4). The ER in eukaryotic cells has four main physiological functions: i) The synthesis of membrane proteins and secretory proteins; ii) the formation of the correct three-dimensional conformation of proteins by folding; iii) the storage of Ca²⁺; and iv) the biology synthesis of lipid and cholesterol. The correct synthesis and secretion of proteins in the ER is regulated by a variety of mechanisms, including the mechanisms by which the oxidative environment, the calcium ion concentration, ATP, protein disulphide isomerase (PDI), heavy-chain binding protein and calprotectin are maintained (1,2,4).

When the ER homeostatic balance is disrupted by a variety of physiological and pathological factors, ER stress (ERS) can be induced in the ER with increased amounts of unfolded and misfolded proteins being formed, calcium depletion and disorder of lipid synthesis (5,6). ERS involves three pathways, namely the unfolded protein response (UPR), Ca²⁺ signaling and ER-related degradation (5-7). They are the main reactionary processes of ERS. ER homeostasis is ultimately achieved through the UPR to reduce the synthesis of novel proteins, to promote folding of unfolded proteins and to increase the degradation of misfolded proteins (1,2,8). In mammalian cells, UPR is mediated by an ER chaperone protein glucose-regulated protein-78/binding immunoglobulin protein (Grp78/Bip) and three ERS-sensing proteins: Protein kinase R-like ER kinase (PERK), inositol-requiring kinase-I (IRE-1) and activating transcription factor 6 (ATF6) (9,10). Bip, which belongs to the family of heat shock protein 70 (HSP70), is a molecular chaperone of the ER, also known as Grp78 (9,10). It serves an important role in the regulation of ERS, and its activation can be used as a marker of the ERS response (11).

Correspondence to: Dr Chaoyang Xu, Department of Thyroid Breast Surgery, Shaoxing People's Hospital, 568 Zhongxing North Road, Shaoxing, Zhejiang 312030, P.R. China
E-mail: ltth53@163.com

Key words: endoplasmic reticulum stress, autophagy, oxidative stress, HepG2, Tunicamycin, Salubrinal

Both PERK and IRE-1 are ER type I transmembrane protein kinases and belong to UPR proximal receptors (1,10).

TF6, an ER type II transmembrane protein kinase, is located on the outside of the ER (12). When the ER is in a state of stress, a large number of unfolded or misfolded proteins accumulate in the ER, while GRP78 dissociates from ATF-6 and PERK-induced proteins and binds to unfolded proteins (12,13). The activation of IRE-1 is unclear, and studies had demonstrated that IRE-1 can be directly activated by unfolded proteins (14). UPR is then simulated by activated free PERK, IRE-1 and ATF6 via their specific pathways, thereby reducing the synthesis of novel proteins and decreasing the accumulation of unfolded and misfolded proteins in the ER to restore the stability of the environment within the ER (12-14).

However, when ERS is too intense or too long, the steady state of ER cannot be restored, UPR can activate the apoptosis signaling pathway to induce apoptosis (15,16). ERS has been previously demonstrated to be a novel way to initiate apoptosis (16). In the early stage of the ERS response, UPR helps to promote cell survival, but if the ERS is too great, the internal environment cannot be restored in time and this leads to apoptosis (16,17). ERS-induced apoptosis is achieved mainly through the following three ways: The activation of transcription factors C/EBP-homologous protein (CHOP)/growth inhibition and DNA damage-inducible gene 153 (GADD153), activation of ASK1/JNK kinase pathway and activation of caspase 12 (18-20). The UPR pathway promotes cell survival and induces apoptosis, however the mechanisms of the transition from pro-survival to pro-apoptotic are unclear (18,20).

Previous studies had demonstrated that autophagy can be induced by ERS through a variety of ways (21,22). From yeasts to mammals, the mutual regulation of ERS and autophagy is a highly conserved process (23). Cell autophagy, also known as type II programmed cell death, had been demonstrated to induce autophagy under conditions of starvation, ERS, hypoxia, and radiation (21,22). In mammalian cells, autophagy is induced by increased levels of PERK, IRE-1 and Ca²⁺ (24). During autophagy, an autophagosome bilayer is formed, which separates the cytosol and proteins from the cytoplasm (25). The outer membrane of the autophagosome then fuses with lysosomes to dissolve the endolyses and their solutes (25). Up to now, >30 autophagy-associated genes have been identified (26,27). These genes are named autophagy-related genes (ATG). The ATG12-ATG5 and LC3-modified ubiquitin-like protein binding systems serve an important role in the formation of autophagosomes in mammals (28,29).

An increasing number of studies have demonstrated that autophagy has an inhibitory effect on tumors and mutations or deletions of related autophagy genes are involved in this process (30,31). A single allelic deletion or mutation of Beclin1 was observed in 40-75% of human breast, ovarian and prostate cancer, and but only a low level of expression occurs in brain tumors (31). In addition, investigations have demonstrated that inhibition of the accumulation of autophagy substrate-p62 can prevent the damage caused by autophagy defects, indicating that autophagy can also inhibit the occurrence of tumors by reducing p62 accumulation (32,33). Other studies revealed that cell autophagy can be induced by high expression of ATG14, resulting in a significant reduction in cell volume and inhibition of tumor growth (34-36).

It has been demonstrated that nutritional deficiencies, ERS and other factors can cause cell autophagy (37). Previous investigations have demonstrated that autophagy caused by starvation causes degradation of a large number of misfolded proteins, but is not specific (37,38). Autophagy caused by anti-neoplastic agents and oxidative stress may be different from starvation because they degrade misfolded proteins through the ubiquitination process (28,29). Therefore, the mechanisms of autophagy induced by drugs or oxidative stress, such as protection or cytotoxicity, and autophagy-regulating cell death, need to be further investigated.

Materials and methods

Cell culture. Human hepatoblastoma cell line HepG2 (39) were purchased from Chinese Academy of Sciences Cell Bank (Shanghai, China). All cells were cultured in Dulbecco's modified Eagle medium (DMEM; Sigma-Aldrich; Merck KGaA, Darmstadt, Germany) containing 10% fetal bovine serum (Sigma-Aldrich; Merck KGaA), 100 U/ml penicillin and 100 µg/ml streptomycin and placed in a cell culture chamber at 37°C and under a humidified atmosphere with 5% CO₂. After the cells adhered and were grown to 80% confluence, the culture medium was removed and washed with appropriate amount of PBS and digested with 0.25% trypsin (Sigma-Aldrich; Merck KGaA). Cells in the logarithmic phase of growth were selected for following experiments.

Cell Counting Kit-8 (CCK-8) assay. The liver cancer cells in the logarithmic growth phase were seeded in 96-well plates at 2x10⁵ cells per well and cultured overnight at 37°C. After the cells were completely adhered and grown to 80% confluence, the culture medium was removed and replaced with culture medium containing different concentrations of H₂O₂ (0, 100, 200, 400, 800 and 1,000 µmol; Sigma-Aldrich; Merck KGaA). After 6, 12, 24 and 48 h with H₂O₂ treatment, 20 µl CCK-8 (Dojindo Molecular Technologies, Inc., Kumamoto, Japan) was added and the cells were cultured at 37°C for another 4 h. The absorption of cell solution was measured at a wavelength of 450 nm.

Reactive oxygen species (ROS) assay. The cells in the logarithmic growth phase were seeded in 96-well plates at 2x10⁵ cells per well and cultured overnight at 37°C. After the cells were grown to 80% confluence, the culture medium was removed and the cells were divided into several groups with medium containing different concentrations of H₂O₂ (0, 200, 400, 600 and 1,000 µmol), respectively. After cultured for another 24 h, cells were harvested, and washed with PBS. Cells were incubated in 20 µM DCFH-DA solution (Sigma-Aldrich; Merck KGaA) at 37°C for 1 h according to manufacturer's protocol. The cells were washed with PBS, ROS production in cells was determined using a flow cytometer (BD Biosciences, Franklin Lakes, NJ, USA). The data was analyzed using FlowJo software version 7.6.1 (FlowJo LLC, Ashland, OR, USA).

Experimental design. The liver cancer cells in logarithmic growth phase were seeded in 96-well plates at 2x10⁵ cells per well and cultured overnight at 37°C. After the cells were completely adhered and grown to 80% confluence, the culture

medium was removed and then the cells were divided into four groups as follows: i) Cells cultured in culture medium without drugs and used as a control; ii), cells cultured in medium containing 600 μmol H_2O_2 and named the H_2O_2 group; iii), cells cultured in medium containing 600 μmol of H_2O_2 and ERS inhibitor Salubrinal (SAL; Sigma-Aldrich; Merck KGaA), and called the H_2O_2 + SAL group; iv), cells cultured in medium containing 600 μmol H_2O_2 and ERS inducer Tunicamycin (TM; Sigma-Aldrich; Merck KGaA), and expressed as H_2O_2 + TM group. After the cells were cultured for 24 h, they were used for the following assays.

Apoptosis detection by flow cytometry. The cells from all groups were harvested and digested, and then were washed twice with PBS and collected at 1×10^5 cells per tube. Apoptosis was detected using a Fluorescein isothiocyanate (FITC) Annexin V Apoptosis Detection kit (BD Biosciences). After 5 μl Annexin V-FITC and 5 μl propidium iodide dyes were added to each well, the cells were incubated at room temperature for 15 min. Then apoptosis was detected by flow cytometry within 1 h. The upper left quadrant represents a mechanically injured cell and the upper right quadrant is a late apoptotic cell. The lower left quadrant is a normal cell and the lower right quadrant is an early apoptotic cell. In this experiment, the proportion of the upper right quadrant + the lower right quadrant was used as the percentage of apoptotic cells. The data was analyzed using FlowJo software version 7.6.1.

Autophagy rate detection by flow cytometry assay. Minimum essential medium (MEM; Gibco; Thermo Fisher Scientific, Inc., Waltham, MA, USA) containing 2 ml monodansylcadaverine (MDC; final concentration 50 NM) was added to each group and incubated for 30 min in a constant temperature incubator at 37°C, 5% CO_2 . The supernatant was collected at 500 x g for 5 min at 4°C. Then the obtained supernatant was discarded and 500 μl MEM containing MDC (final concentration of 50 NM) was added to each group and then incubated at 37°C for 30 min. Cells were washed twice with PBS and digested with 0.25% trypsin for 2 min, then 1 ml PBS was added and mixed. The cells obtained were then collected in 1.5 ml centrifuge tubes and centrifuged at 500 x g for 5 min at 4°C. The supernatants were discarded, 1 ml PBS was added to re-suspend the supernatant. The solutions were then centrifuged at 500 x g for 5 min at 4°C. A total of 800 μl supernatant was sucked out and the remaining 200 μl was mixed. The fluorescence intensity of MDC staining of the solution obtained was measured on a flow cytometer at an excitation wavelength of 488 nm after passing a 300 mesh copper mesh. The data was analyzed using FlowJo software version 7.6.1.

Western blotting assay. Buffer A cell lysates (Cell Signaling Technology Inc., Danvers, MA, USA) containing a protease and phosphatase inhibitor cocktail (Roche Diagnostics, Basel, Switzerland) were added to the cells collected from all groups, and homogenized for 30 min at 4°C. Total protein extracts were quantified by Bicinchoninic acid Protein Assay kit (Thermo Fisher Scientific, Inc.). Proteins (30 μg) were separated by 10% SDS-PAGE and then transferred to a nitrocellulose membrane. Subsequently, the membranes were blocked with 5% fat-free dry milk at room temperature for 1 h. Following

this, the blots were incubated with human anti-GRP78 (cat. no. ab181499; Abcam, Cambridge, MA, USA; 1:1,000), anti-IRE1 (cat. no. ab48187, Abcam; 1:2,000), anti-ATF6 (cat. no. ab37149; Abcam; 1:1,000), anti-CHOP (cat. no. ab11419; Abcam; 1:1,000), anti-pro caspase-3 (cat. no. ab32150; Abcam; 1:1,000), anti-pro caspase-9 (cat. no. ab135544; Abcam; 1:500), anti-caspase-12 (cat. no. ab62484; Abcam; 1:1,000), anti-p62 (cat. no. ab56416; Abcam; 1:500), anti- β -actin (cat. no. ab8226; Abcam; 1:2,000) overnight at 4°C. The membranes were again washed with PBS and incubated with horseradish peroxidase (HRP)-conjugated goat anti-rabbit IgG secondary antibodies (cat. no. P0448; Dako; Agilent Technologies, Inc., Santa Clara, CA, USA; 1:2,000) at room temperature for 1 h. The proteins were finally examined by an enhanced chemiluminescence system (ECL) (Bio-Rad Laboratories, Inc., Hercules, CA, USA). Band intensities were quantified by densitometry using ImageJ Software version 1.6 (National Institutes of Health, Bethesda, MD, USA).

Reverse transcription-quantitative polymerase chain reaction (RT-qPCR) assay. Total RNA from cells was extracted using the RNeasy mini-kit (Qiagen GmbH, Hilden, Germany) according to manufacturer's protocol. Total RNA (1 μg) was reverse-transcribed with an iScript cDNA Synthesis kit (Bio-Rad Laboratories, Inc.), according to the manufacturer's protocol. Primers were synthesized by Sangon Biotech Co., Ltd., (Shanghai, China). Relative quantification of mRNA was performed by qPCR using iQ SYBR-Green Supermix and iCycler iQ thermal cycler (Bio-Rad Laboratories, Inc.). The thermocycling conditions were as follows: 95°C for 10 min, followed by 40 cycles of 95°C for 15 sec, 60°C for 60 sec, and 72°C for 60 sec. Each sample was determined in duplicate. All PCR products were confirmed by 1.5% agarose gel electrophoresis. Data were calculated using the $2^{-\Delta\Delta\text{Ct}}$ method (40) and relative expression was normalized to an endogenous reference (β -actin). Primers were as follows: GRP78: 5'-GAGTAG GCGACGGTGAGGTC-3' (forward) and 5'-GAGCACAGC GCAATTTCCGA-3' (reverse); IRE1: 5'-GCTCCAGAGATG CTGAGCGA-3' (forward) and 5'-GTGCTTCTCTGGGTG CAAGC-3' (reverse); p50ATF6: 5'-AGAGGCAACCCACGT TGTCA-3' (forward) and 5'-GCCACCAAGGCAGAAAGC AG-3' (reverse); CHOP: 5'-TGCAGAGATGGCAGCTGAGT-3' (forward) and 5'-CCAAGCCAGAGAAGCAGGGT-3' (reverse); β -actin: 5'-GGCACTCTTCCAGCCTTCT-3' (forward) and 5'-GCACTGTGTTGGCGTACAGG-3' (reverse).

Statistical analysis. The results are expressed as the mean \pm standard deviation of the mean of three independent experiments. Statistical comparisons between different groups were conducted by with SPSS software (version 20; IBM Corps., Armonk, NY, USA). Two-tailed one-way analysis of variance followed by Bonferroni post hoc pairwise comparison was used to assess the differences between groups. $P < 0.05$ was considered to indicate a statistically significant difference.

Results

Cell viability is affected by H_2O_2 in a dosage- and time-dependent manner. To test the consequences of increased oxidative stress on the cell viability of human hepatoblastoma cell line HepG2,

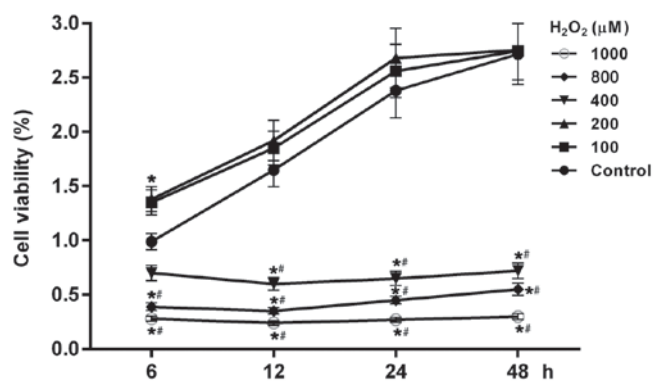


Figure 1. Cell viability was significantly influenced by H₂O₂ treatment. Cell Counting Kit-8 assay demonstrated that cell viabilities were affected in a dosage- and time-dependent manner. With increased treatment time, cell viabilities were increased in cells treated with low concentrations of H₂O₂ (100 and 200 μmol), and decreased in cells presented in high concentrations of H₂O₂ (400, 800 and 1,000 μmol). *P<0.05 vs. the control group; #P<0.05 vs. 100 or 200 μmol H₂O₂.

cells were incubated in different concentrations of H₂O₂ (0, 100, 200, 400, 800 and 1,000 μmol). The results demonstrated that cell viability in all groups altered in a dose- and time-dependent manner (Fig. 1). As well as in the control group, cell viability in groups with 100 and 200 μmol H₂O₂ increased with increased time (Fig. 1). While in the group with the higher concentrations of H₂O₂ (400, 800 and 1,000 μmol), cell viability was significant reduced compared with the control and cells treated with low concentration of H₂O₂ (100 and 200 μmol; P<0.05). In groups with high concentration treatments of H₂O₂, cell viability was lowest at 12 h following cell treatment with H₂O₂, suggesting that cell growth or cell apoptosis were affected by high oxidative stress.

ROS levels in cells treated with H₂O₂ are increased in a dosage-dependent manner. Cell viability was affected by H₂O₂ treatments, indicating that cell damage was induced by oxidative stress. Therefore, the ROS levels induced by different concentrations of H₂O₂ were measured. The flow cytometry assay demonstrated that ROS levels were significantly elevated with increased treatment concentrations of H₂O₂ (P<0.05; Fig. 2). The ROS levels in cells treated with 600 and 1,000 μmol H₂O₂ were ~10 and 15 fold of that of control, respectively (Fig. 2). Hence, together with the results of cell viability test, the cells treated with 600 μmol H₂O₂ had moderate injuries; therefore this dose was chosen for the oxidative damage model and used in subsequent experiments.

Increased apoptosis and cell autophagy rates induced by H₂O₂ are significantly affected by SAL and TM. To examine apoptosis and cell autophagy rates in cells with ERS induced by oxidative stress, cells were treated with H₂O₂ + ER inhibitor SAL and ERS inducer TM. Compared with the control, apoptosis rates were significantly increased in groups treated with H₂O₂ (P<0.05; Fig. 3). However, compared with cells treated with H₂O₂ alone, the apoptosis rates were decreased and increased in cells treated with H₂O₂ + SAL and with H₂O₂ + TM, respectively (P<0.05; Fig. 3).

Similarly, cell autophagy rates were significantly increased in all groups compared with the control (P<0.05; Fig. 4).

Compared with cells treated with H₂O₂ alone, cell autophagy rates were significantly decreased and increased in cells with H₂O₂ + SAL and H₂O₂ + TM treatments, respectively (P<0.05; Fig. 4).

SAL and TM treatment can reduce and increase the expression of ERS associated genes, respectively. To further investigate the effects of H₂O₂, SAL and TM on ERS, the expression of ERS-associated genes were determined. As demonstrated in Fig. 5, a western blot assay revealed that the expression levels of GRP78, IRE1, p50ATF6 and CHOP proteins were significantly increased following treatment with H₂O₂, compared with the control (P<0.05). The expression level of the aforementioned genes decreased and increased in cells treated with H₂O₂ + SAL and H₂O₂ + TM, respectively, compared with the cells treated with H₂O₂ alone (Fig. 5A and B).

Similarly, mRNA expression levels of GRP78, IRE1, p50ATF6 and CHOP were upregulated in cells treated with H₂O₂ alone and with H₂O₂ + TM, compared with the control (P<0.05). However, the mRNA expression levels were significantly downregulated and upregulated in cells treated with H₂O₂ + SAL and H₂O₂ + TM, respectively compared with cells treated with H₂O₂ alone (P<0.05; Fig. 5C).

TM stimulates the upregulation of apoptosis-related genes of ER pathway and autophagy. Previous tests revealed that apoptosis and autophagy were induced following treatment with H₂O₂ and TM. Consequently, the expression of apoptosis genes and cell autophagy-associated genes were measured. The results demonstrated that the protein expression levels of pro caspase-3 and pro caspase-9 were significantly decreased in the cells treated with H₂O₂ alone and with H₂O₂ + TM, compared with the control (P<0.05; Fig. 6). They were increased and decreased in the cells treated with H₂O₂ + SAL and with H₂O₂ + TM, respectively, compared with the cells treated with H₂O₂ alone (P<0.05; Fig. 6). By contrast, the protein levels of caspase-12 were significantly increased in cells treated with H₂O₂, compared with the control (P<0.05). The protein levels were downregulated and upregulated in cells treated with H₂O₂ + SAL and with H₂O₂ + TM, respectively, compared with the cells treated with H₂O₂ alone (Fig. 6A and B).

The expression levels of LC3-I and LC3-II protein were increased in cells treated with H₂O₂ and with H₂O₂ + TM, compared with the control. The levels of LC3-I and LC3-II protein were downregulated and upregulated in cells treated with H₂O₂ + SAL and with H₂O₂ + TM, compared with cells treated with H₂O₂ alone, respectively. By contrast, the levels of p62 protein were significantly downregulated after cells were treated with H₂O₂ (P<0.05; Fig. 6C and D). Compared with cells treated with H₂O₂ alone, the expression levels of p62 protein were increased and reduced, respectively in cells treated with H₂O₂ + SAL and with H₂O₂ + TM. These results confirmed the observation of increased autophagy rates detected by flow cytometry assay, indicating that the formation of autophagosomes was increased in cells treated with H₂O₂ or H₂O₂ + TM.

Discussion

The present study investigated the role of ERS-autophagy on the oxidative damage induced by H₂O₂ and the mechanism

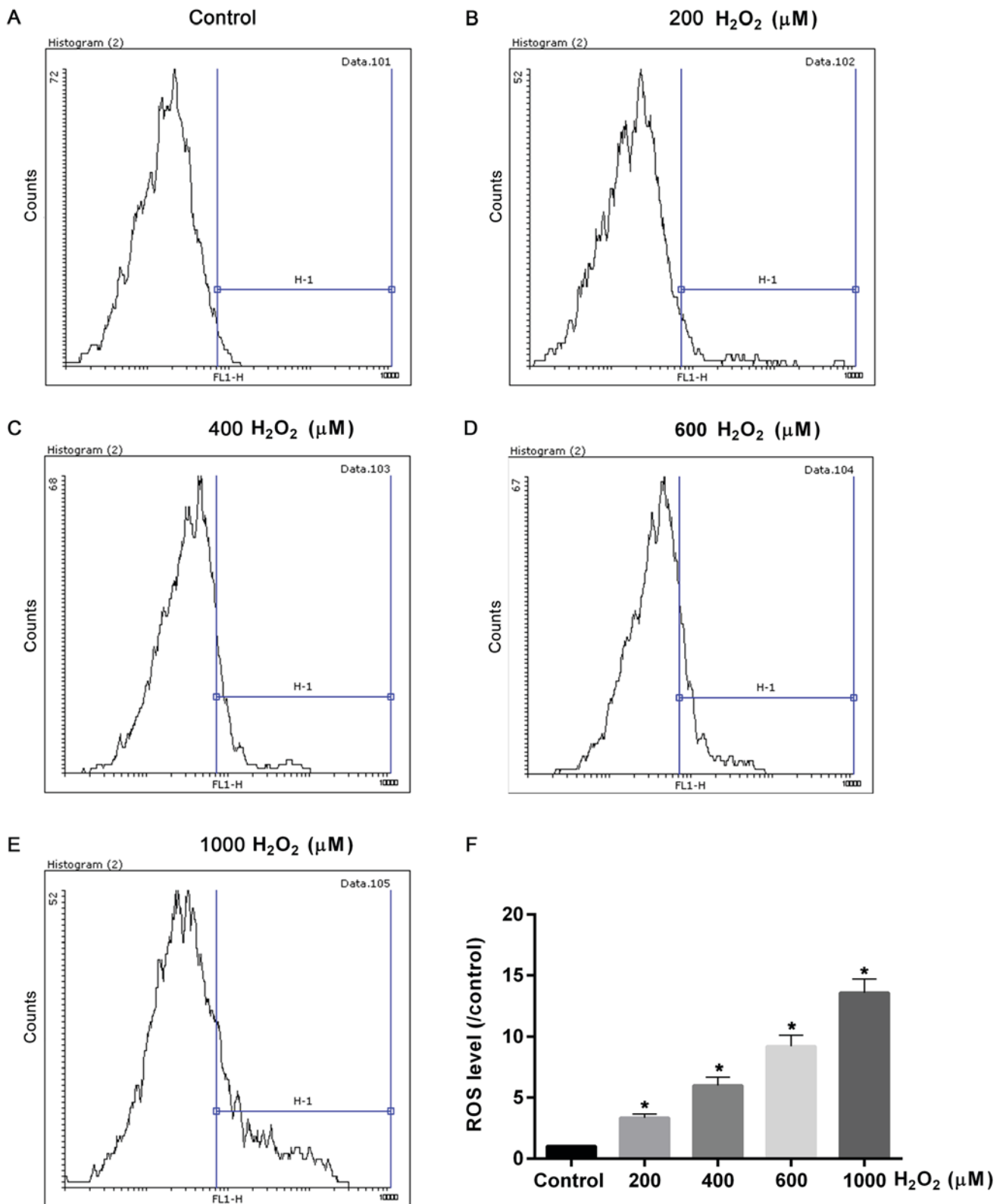


Figure 2. ROS levels in cells induced by H₂O₂ were elevated in a dosage-dependent manner. Flow cytometry assay demonstrated that ROS levels were increased with treatment concentrations of H₂O₂ in the (A) control, (B) 200, (C) 400, (D) 600 and (E) 1,000. (F) Relative levels of ROS were significantly increased in the dosage of H₂O₂ dependent manner. *P < 0.05 vs. the control group. ROS, reactive oxygen species.

involved. The present study demonstrated that oxidative damage induced by H₂O₂ can be inhibited and enhanced by the ERS inhibitor SAL and inducer TM, respectively. Furthermore, TM treatment increased apoptosis and autophagy rates, indicating that ERS-autophagy is involved in the apoptosis of HepG2

cells. In addition, these processes were inhibited by the ERS inhibitor SAL, confirming the role of ERS-autophagy on the apoptosis induced by oxidative stress. Consistent with these observations, TM increased the expression of ERS-associated genes, including GRP78, IRE1, p50ATF6 and CHOP, and also

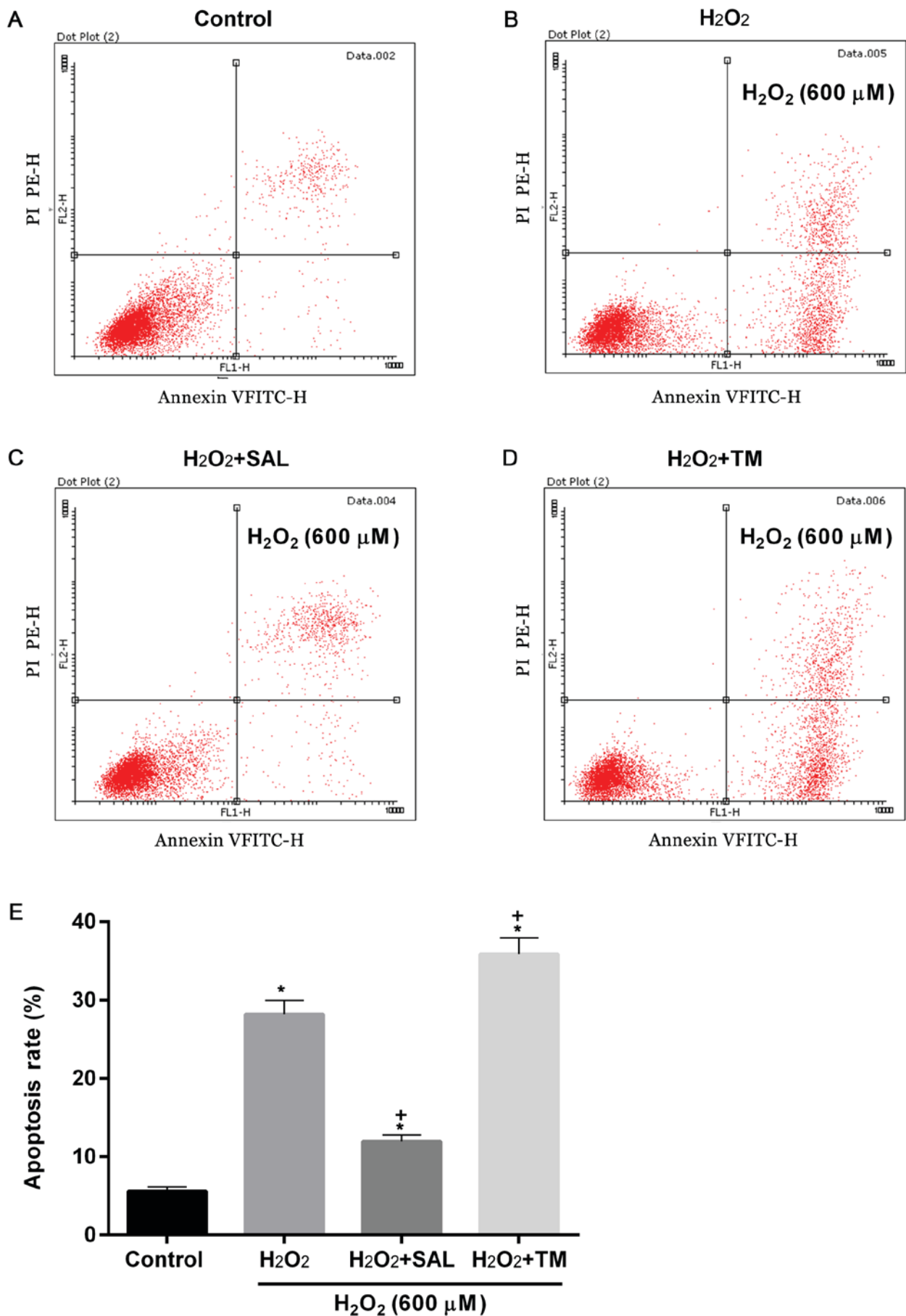


Figure 3. Apoptosis rates induced by H₂O₂ were significantly affected by SAL and TM. (A-D) Apoptosis rates were determined by flow cytometry. (E) The results demonstrated that apoptosis rates were simulated by treatment of H₂O₂, which were reduced and increased in cells treated with SAL and TM, respectively. *P<0.05 vs. the control group; †P<0.05 vs. the H₂O₂ group. TM, Tunicamycin; SAL, Salbrinal; FITC, fluorescein isothiocyanate; PI, propidium iodide.

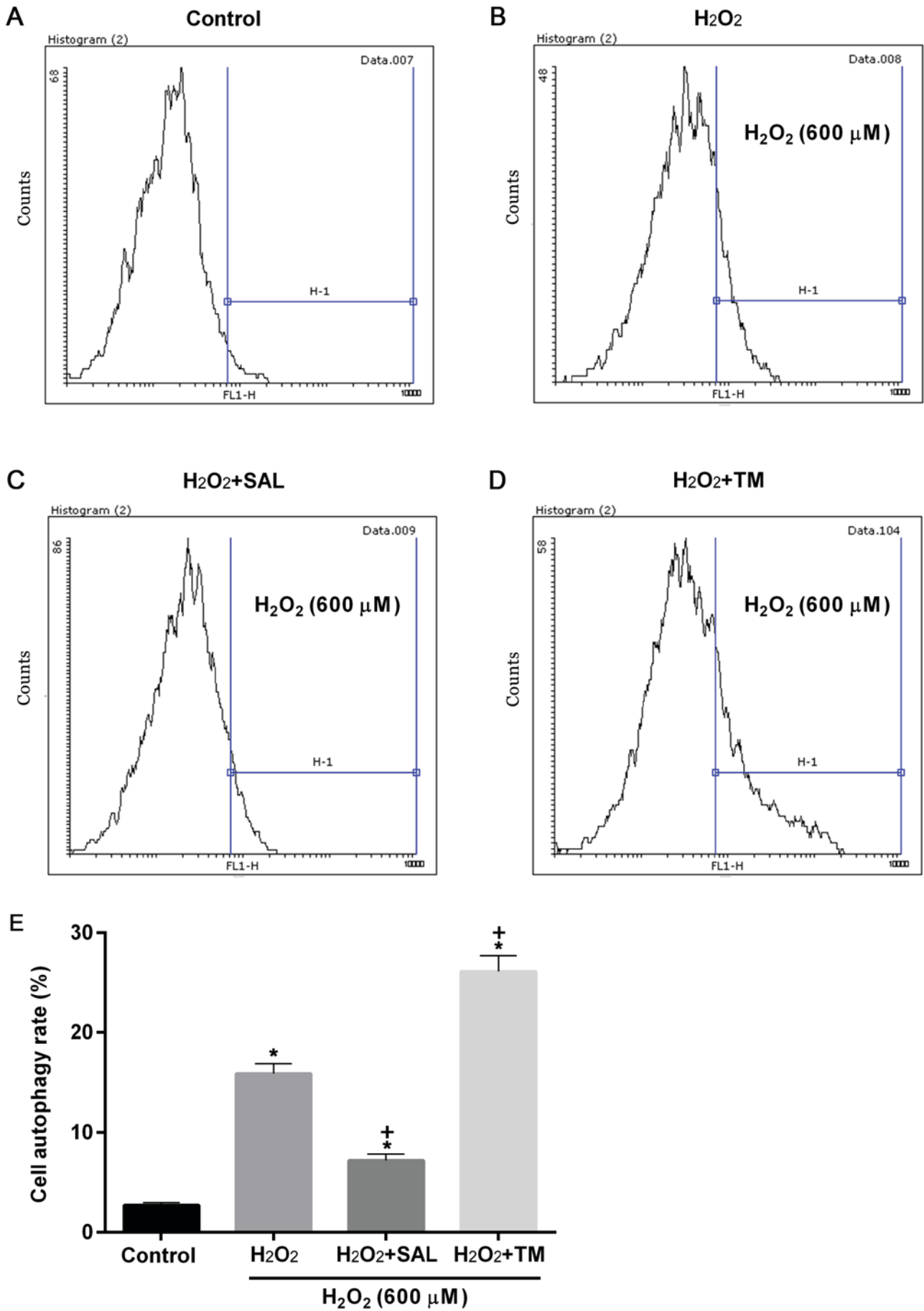


Figure 4. Cell autophagy rates induced by H₂O₂ were significantly affected by SAL and TM. (A-D) Cell autophagy rates were detected by flow cytometry. (E) The results demonstrated that cell autophagy rates were simulated in cells treated with H₂O₂, which were reduced and increased in cells treated with SAL and TM, respectively. *P<0.05 vs. the control group. +P<0.05 vs. the H₂O₂ group. TM, Tunicamycin; SAL, Salbrinal.

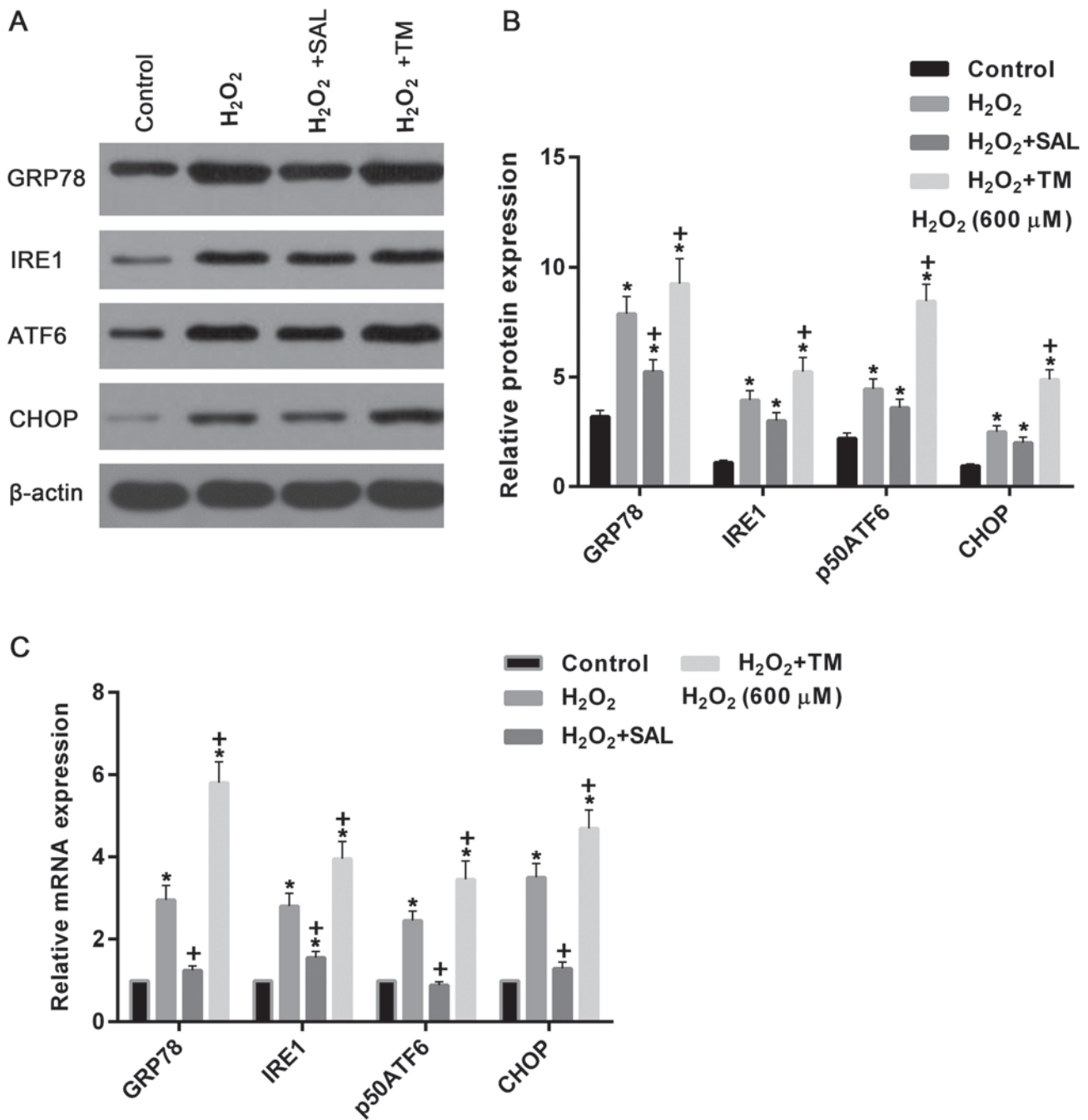


Figure 5. Expression levels of ERS-associated proteins were simulated by H₂O₂ and TM, and inhibited by SAL. (A) Western blot assay and (B) quantification of the assay measuring the expression levels of GRP78, IRE1, p50ATF6 and CHOP proteins were increased in cells with H₂O₂ treatment. Compared with cells treated with H₂O₂ alone, they were reduced and increased in cells treated with H₂O₂ + SAL and H₂O₂ + TM, respectively. (C) Reverse transcription-quantitative polymerase chain reaction assay demonstrated that expression levels of GRP78, IRE1, p50ATF6 and CHOP mRNA were increased in cells treated with H₂O₂ alone and with H₂O₂ + TM, compared with the control. These repression levels were significantly reduced and increased in cells treated with H₂O₂ + SAL and H₂O₂ + TM, compared with cells treated with H₂O₂ alone, respectively. *P<0.05 vs. the control group. **P<0.05 vs. the H₂O₂ group. TM, Tunicamycin; SAL, Salbrinal; ERS, endoplasmic reticulum stress; CHOP, C/EBP-homologous protein; IRE1, inositol-requiring kinase-I; GRP78, glucose-regulated protein-78; ATF6, activating transcription factor 6.

the expression of autophagy-associated genes LC3-I, LC3-II and p62.

Primary and secondary resistance remains a bottleneck in the clinical treatment of cancer (41). The mechanism of the formation of drug-resistant tumor cells is not only associated with the increased expression of resistance and anti-apoptotic genes of tumor cells, but also the results of the present study suggest that autophagy, ERS and other signaling pathways are

involved in the formation of drug resistance mechanisms of tumor cells (42,43). ERS and autophagy are adaptive responses of cells to injury stimuli (43). ERS-induced autophagy can maintain homeostasis of the intracellular environment, serving a certain protective role (43). When ERS occurs, the UPR can activate autophagy and subsequently autophagy can reduce the load of the ER by degrading the misfolded or unfolded protein and suppressing the excessive activation of ERS (5,43).

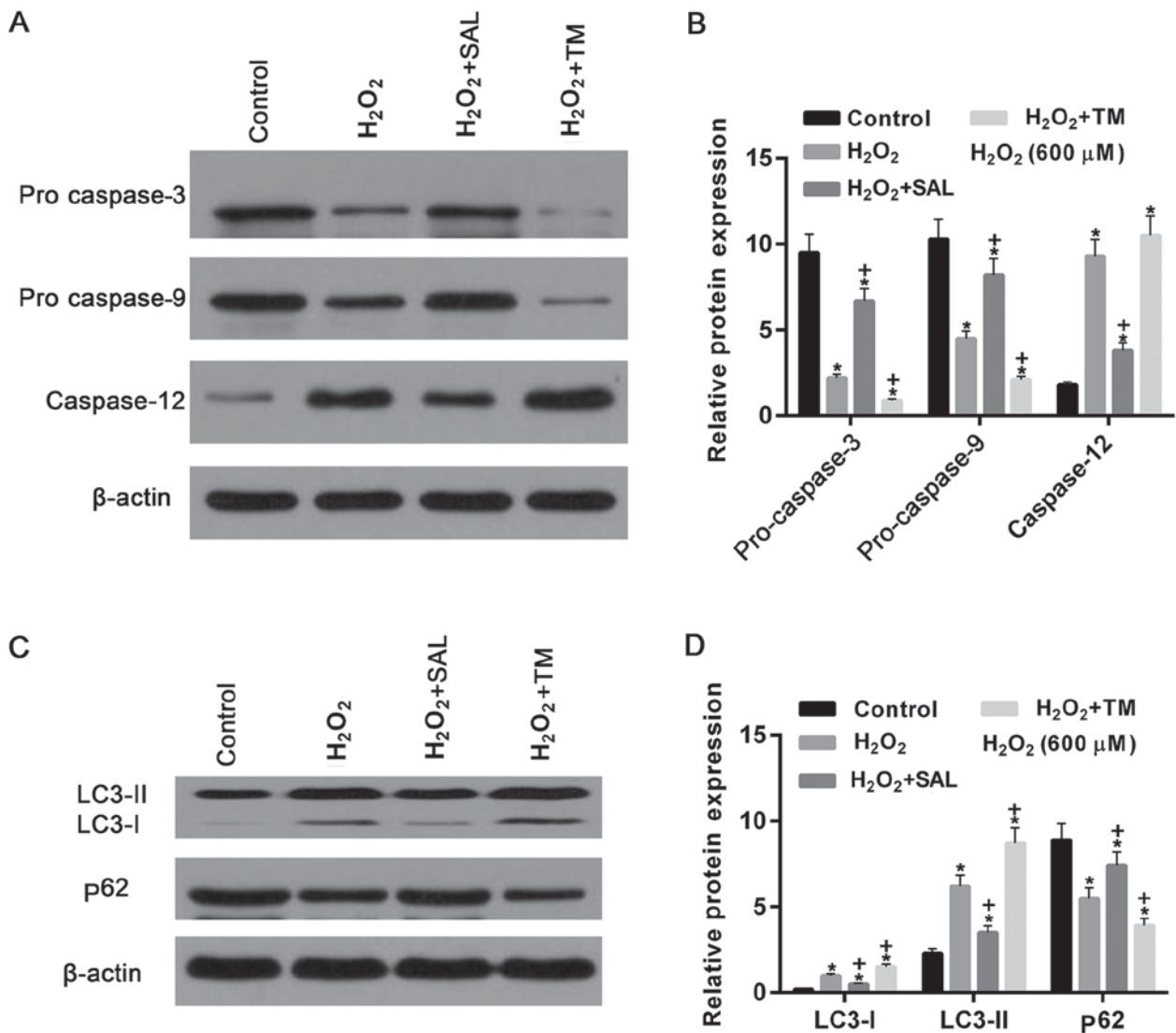


Figure 6. Apoptosis- and cell autophagy-associated genes in cells treated with H₂O₂ were significantly altered following co-treatment with SAL and TM. (A) Western blot assay and (B) quantification of the results demonstrated that the expression of pro caspase-3 and pro caspase-9 were decreased following cells treated with H₂O₂, compared with the control. Compared with the cells treated with H₂O₂ alone, they were increased and decreased in cells treated with H₂O₂ + SAL and with H₂O₂ + TM, respectively. However, caspase-12 was significantly increased in cells treated with H₂O₂. They were reduced and increased in cells treated with H₂O₂ + SAL and with H₂O₂ + TM, compared with cells treated with H₂O₂ alone, respectively. (C) Western blotting and (D) quantification of the western blot. The levels of LC3-I, LC3-II protein were increased in cells treated with H₂O₂ alone. Protein levels of LC3-I, LC3-II were decreased and increased in cells treated with H₂O₂ + SAL and with H₂O₂ + TM, compared with cells treated with H₂O₂ alone, respectively. By contrast, the expression levels of p62 protein were decreased by H₂O₂ treatment compared with the control group, and upregulated and downregulated in cells treated with H₂O₂ + SAL and with H₂O₂ + TM, compared to cells treated with H₂O₂ alone, respectively. *P<0.05 vs. control group. ⁺P<0.05 vs. H₂O₂ group. TM, Tunicamycin; SAL, Salbrinal.

In addition, degradation products produced by these processes also provide the raw material for the synthesis of novel proteins in the cell, the reconstruction of the cell structure and the formation of ATP (15,17).

However, the over-activation of ERS can increase cell damage and even cause cell death (19,20,44). The present study investigated the association between oxidative stress, the ERS inhibitor SAL and ERS inducer TM to identify the effect of ERS on oxidative damage induced by H₂O₂ in the liver cancer cell line HepG2 and its mechanism. The results of the present study demonstrated that oxidative damage induced by H₂O₂ can be increased by TM-induced ERS, which was confirmed by the elevations of apoptosis and autophagy rates. It also demonstrated that ERS was induced in cells treated with a high concentration of H₂O₂ (600 μM), which can be

attenuated in cells treated with the ER inhibitor SAL, resulting in a reduction of apoptosis and autophagy rates. These results suggested that ER inducer can enhance oxidative stress damage in HepG2 cells.

The subsequent experiments revealed that the expression levels of ERS-related genes, such as GRP78, IRE1, p50ATF6 and CHOP, were increased in cells treated with TM + H₂O₂, compared with cells treated with H₂O₂ alone. It is well known that in the absence of ERS, the N-terminus of IRE1, p50ATF6 and PERK binds to the chaperone Grp78/Bip and they are present in inactive state (6,11). When ERS occurs, a large number of unfolded proteins accumulate in the ER cavity, IRE1, p50ATF6 and PERK are then separated from Grp78/Bip, and Grp78/Bip binds to the unfolded proteins (11,14,24). ERS-regulated apoptosis is mediated

by activation of the transcription factor CHOP/GADD153, the apoptotic signaling kinase 1 (ASK1)/c-Jun N-terminal kinase 1 (JNK) kinase pathway and caspase 12 (19). CHOP, also known as GADD153, is a member of the C/EBP transcription factor family and is a specific transcription factor for ERS (18,19). When the ERS occurs, activated PERK, IRE-1 and p50ATF6 can elevate CHOP expression, and ultimately activate caspase 3 to induce apoptosis (18,19,45). Consistent with this mechanism, the results in present study demonstrated that the elevation of CHOP expression and the reduction of pro-caspase 3 level were observed when the upregulation of IRE-1 and p50ATF6 were induced by ERS. In addition, when IRE-1 is activated, it can bind to tumor necrosis factor receptor factor 2 (TRAF2) and ASK1 to form IRE1/TRAF2/ASK1 complex, and further activate JNK, which finally results in apoptosis (14,46). Furthermore, a number of studies had revealed that activated calpain kinase can activate caspase 12 when ERS is activated by an imbalance in intramolecular calcium storage, whereas activated PERK and IRE-1 can also further activate caspase-12 by activating TRAF2 protein (14,46,47). Activated caspase-12 is then transferred to the cytoplasm, causing the caspase-9 precursors to cleave and activate caspase-9 to activate caspase-3, leading to apoptosis, whereas this pathway does not depend on mitochondria (48). The results revealed that caspase-12 was increased and levels of pro caspase-3 were reduced, indicating that ERS-induced apoptosis is involved in CHOP/GADD153, the ASK1/JNK kinase and caspase 12 pathway in HepG2 cells. In addition, the present study demonstrated that the ERS inducer TM can enhance the apoptosis of HepG2 cells induced by H₂O₂ via elevating ERS.

Previously, it has been demonstrated that starvation, ERS and other factors can induce cell autophagy (37). Similar to a number of investigations, the results of the present study demonstrated that cell autophagy was stimulated by ERS (37,49). Previous studies have demonstrated that two ubiquitin-like binding systems are involved in the formation of autophagosomes (37,49). One is the AtgS/Atg 12 system, including Atg5, Atg 12, Atg7, Atg 10 and Atg 16 (29,49). The other ubiquitin-like binding system is comprised of LC3/Atg8 and its targeted molecular phosphatidylethanolamine (PE) (49,50). With the help of Atg 4, Atg 7 and Atg 3, part of the amino acid residue at the carboxy terminus of LC3/Atg8 is first cleaved to reveal the end of the aminoacetic acid, and then LC3/Atg8 and PE are bound to each other through a dialkylamine bond (49,50). Following binding, LC3/Atg 8 are transformed from type I, which is dispersed in the cytoplasm, to type II, which is localized on the autophagic membrane (49,50). Therefore, an increase in LC3-II expression is considered to be a marker of autophagy (50,51). However, in the present study no statistical differences were found for the ratio of LC3-II and LC-I between different groups (data not shown). ERS involves the whole process of protein synthesis, it can also induce the expression of LC3 II and Beclin 1 to promote the formation of autophagosomes (52). However, the specific mechanism of ERS in autophagy of tumor cells is not very clear. Previous studies suggested that ERS induced by overexpression of mutant proteins can induce the activation of autophagy, which is mediated in part by the PERK/eIF2a pathway (53-55). At the molecular level, elevated levels of autophagy by PERK may be

mediated by the upregulation of autophagy-related gene Atg 12 (45,55). Therefore, autophagy is a defense mechanism of cells against misfolded proteins and this process is regulated by UPR. Researchers also demonstrated that the formation of LC3 autophagosomes is dependent on the IRE-1 pathway, but not by the PERK pathway (56). Notably, autophagy activation occurs through IRE-1 kinase activity rather than endonuclease activity and IRE-1 activates the TRAF2/JNK pathway to activate autophagy (57,58). The results demonstrated that LC3 II protein expression was increased in cells treated with H₂O₂ alone and with TM + H₂O₂, indicating that autophagy was induced by oxidative stress and TM, and the latter enhanced the former. Furthermore, activation of autophagy helps cells clear ubiquitinated proteins by p62 (33). When autophagy occurs, p62 is bound to the autophagy factor ATG8/LC3 by its ubiquitin-associated region at the C-terminus interacting with the LC3-interacting region of LC3 and is transferred to the autophagosome and then is degraded (33,59). Studies demonstrated that the misfolding of the proteins produced in the cell may first be ubiquitinated and then degraded by the p62 autophagy pathway, decreasing ERS (33,60). The present study also revealed that in cells treated with H₂O₂ alone and with TM + H₂O₂, p62 expression was downregulated, and LC3 II expression was upregulated, compared with the control and cells treated with SAL + H₂O₂. Together with the elevation of autophagy rates in cells treated with H₂O₂ alone and with TM + H₂O₂, it is hypothesized that autophagy can be induced by H₂O₂ and enhanced by ER.

In conclusion, ERS and autophagy can be triggered by H₂O₂, which can stimulate apoptosis of the liver cancer cell line HepG2 when cells are exposed to high concentrations of H₂O₂. The results suggested that ERS inducer TM may be a potential target for treating oxidative stress damage of tumor cells induced by antitumor drugs via enhancing ERS and autophagy.

Acknowledgements

Not applicable.

Funding

No funding was received.

Availability of data and materials

The analyzed data sets generated during the study are available from the corresponding author on reasonable request.

Authors' contributions

ZW, HW and CX designed the experiments. ZW and SF performed the experiments. ZW, HW and SF analyzed the data. ZW, HW and SF wrote the manuscript. ZW and HW revised the manuscript. All authors reviewed the manuscript.

Ethics approval and consent to participate

Not applicable.

Patient consent for publication

Not applicable.

Competing interests

The authors declare they have no competing interests.

References

1. Benham AM: Protein folding and disulfide bond formation in the eukaryotic cell: Meeting report based on the presentations at the European Network Meeting on Protein Folding and Disulfide Bond Formation 2009 (Elsinore, Denmark). *FEBS J* 276: 6905-6911, 2009.
2. Kato H and Nishitoh H: Stress responses from the endoplasmic reticulum in cancer. *Front Oncol* 5: 93, 2015.
3. Henderson KA: Boric acid localization and effects on storage calcium release and the endoplasmic reticulum in prostate cancer cells. *Dissertations & Theses-Gradworks*, 2009.
4. Schapansky J, Morissette M, Odero G, Albensi B and Glazner G: Neuregulin beta1 enhances peak glutamate-induced intracellular calcium levels through endoplasmic reticulum calcium release in cultured hippocampal neurons. *Can J Physiol Pharmacol* 87: 883-891, 2009.
5. Mandl J, Mészáros T, Bánhegyi G and Csala M: Minireview: Endoplasmic reticulum stress: Control in protein, lipid, and signal homeostasis. *Mol Endocrinol* 27: 384-393, 2013.
6. Rangelaldao R: The unfolded protein response, inflammation, oscillators, and disease: A systems biology approach. *Endo Retikulum Stress Dis* 2: 30-52, 2015.
7. Richie DL, Feng X, Hartl L, Aimaniananda V, Krishnan K, Powers-Fletcher MV, Watson DS, Galande AK, White SM, Willett T, *et al*: The virulence of the opportunistic fungal pathogen requires cooperation between the endoplasmic reticulum-associated degradation pathway (ERAD) and the unfolded protein response (UPR). *Virulence* 2: 12-21, 2011.
8. Townsend DM, Manevich Y, He L, Xiong Y, Bowers RR Jr, Hutchens S and Tew KD: Nitrosative-stress induced S-glutathionylation of PDI leads to activation of the unfolded protein response. *Cancer Res* 69: 7626-7634, 2009.
9. Reddy RK, Mao C, Baumeister P, Austin RC, Kaufman RJ and Lee AS: Endoplasmic reticulum chaperone protein GRP78 protects cells from apoptosis induced by topoisomerase inhibitors: Role of ATP binding site in suppression of caspase-7 activation. *J Biol Chem* 278: 20915-20924, 2003.
10. Bennett HL, Fleming JT, O'Prey J, Ryan KM and Leung HY: Androgens modulate autophagy and cell death via regulation of the endoplasmic reticulum chaperone glucose-regulated protein 78/BiP in prostate cancer cells. *Cell Death Dis* 1: e72, 2010.
11. Lu T, Yang W, Wang Z, Hu Z, Zeng X, Yang C, Wang Y, Zhang Y, Li F, Liu Z, Wang D and Ye Z: Knockdown of glucose-regulated protein 78/binding immunoglobulin heavy chain protein expression by asymmetric small interfering RNA induces apoptosis in prostate cancer cells and attenuates migratory capability. *Mol Med Rep* 11: 249, 2015.
12. Maiuolo J, Bulotta S, Verderio C, Benfante R and Borgese N: Selective activation of the transcription factor ATF6 mediates endoplasmic reticulum proliferation triggered by a membrane protein. *Proc Natl Acad Sci USA* 108: 7832-1837, 2011.
13. Umabayashi K, Hirata A, Horiuchi H, Ohta A and Takagi M: Unfolded protein response-induced BiP/Kar2p production protects cell growth against accumulation of misfolded protein aggregates in the yeast endoplasmic reticulum. *Eur J Cell Biol* 78: 726-738, 1999.
14. Gardner BM and Walter P: Unfolded proteins are Ire1-activating ligands that directly induce the unfolded protein response. *Science* 333: 1891-1894, 2011.
15. Tang J, Guo YS, Zhang Y, Yu XL, Li L, Huang W, Li Y, Chen B, Jiang JL and Chen ZN: CD147 induces UPR to inhibit apoptosis and chemosensitivity by increasing the transcription of Bip in hepatocellular carcinoma. *Cell Death Differ* 19: 1779-1790, 2012.
16. Hiss DC and Gabriels GA: Implications of endoplasmic reticulum stress, the unfolded protein response and apoptosis for molecular cancer therapy. Part II: Targeting cell cycle events, caspases, NF- κ B and the proteasome. *Exp Opin Drug Discov* 4: 907-921, 2009.
17. Svetlana S, Patricia C, Mnich K, Ayo A, Pakos-Zebrucka K, Patterson JB, Logue SE and Samali A: Endoplasmic reticulum stress-mediated induction of SESTRIN 2 potentiates cell survival. *Oncotarget* 7: 12254-12266, 2016.
18. Netherton CL, Parsley JC and Wileman T: African swine fever virus inhibits induction of the stress-induced proapoptotic transcription factor CHOP/GADD153. *J Virol* 78: 10825-10828, 2004.
19. Moriya S, Miyazawa K, Kawaguchi T, Che XF and Tomoda A: Involvement of endoplasmic reticulum stress-mediated CHOP (GADD153) induction in the cytotoxicity of 2-aminophenoxazine-3-one in cancer cells. *Int J Oncol* 39: 981-988, 2011.
20. Tan Y, Dourdin N, Wu C, De VT, Elce JS and Greer PA: Ubiquitous calpains promote caspase-12 and JNK activation during endoplasmic reticulum stress-induced apoptosis. *J Biol Chem* 281: 16016-16024, 2006.
21. Niso-Santano M, Bravo-San Pedro JM, Gómez-Sánchez R, Climent V, Soler G, Fuentes JM and González-Polo RA: ASK1 overexpression accelerates paraquat-induced autophagy via endoplasmic reticulum stress. *Toxicol Sci* 119: 156, 2011.
22. Nakka VP, Prakash-Babu P and Vemuganti R: Crosstalk between endoplasmic reticulum stress, oxidative stress, and autophagy: Potential therapeutic targets for acute CNS injuries. *Mol Neurobiol* 53: 532-544, 2016.
23. Devenish RJ and Klionsky DJ: Autophagy: Mechanism and physiological relevance 'brewed' from yeast studies. *Front Biosci (Schol Ed)* 4: 1354-1363, 2012.
24. Deegan S, Koryga I, Glynn SA, Gupta S, Gorman AM and Samali A: A close connection between the PERK and IRE arms of the UPR and the transcriptional regulation of autophagy. *Biochem Biophys Res Commun* 456: 305-311, 2015.
25. Drake KR, Kang M and Kenworthy AK: Nucleocytoplasmic distribution and dynamics of the autophagosome marker EGFP-LC3. *PLoS One* 5: e9806, 2010.
26. Tamura H, Shibata M, Koike M, Sasaki M and Uchiyama Y: Atg9A, an autophagy-related membrane protein, is localized in neurons of mouse brain. *Neuroscience Research* 68: 443-453, 2010.
27. Jo YK, Kim SC, Park IJ, Park SJ, Jin DH, Hong SW, Cho DH and Kim JC: Increased expression of ATG10 in colorectal cancer is associated with lymphovascular invasion and lymph node metastasis. *PLoS One* 7: e52705, 2012.
28. Chen ZH, Cao JF, Zhou JS, Liu H, Che LQ, Mizumura K, Li W, Choi AM and Shen HH: Interaction of caveolin-1 with ATG12-ATG5 system suppresses autophagy in lung epithelial cells. *Am J Physiol Lung Cell Mol Physiol* 306: 1016-1025, 2014.
29. Hwang S, Maloney NS, Bruinsma MW, Goel G, Duan E, Zhang L, Shrestha B, Diamond MS, Dani A, Sosnovtsev SV, *et al*: Nondegradative role of Atg5-Atg12/ Atg16L1 autophagy protein complex in antiviral activity of interferon gamma. *Cell Host Microbe* 11: 397-409, 2012.
30. Kung CP, Budina A, Balaburski G, Bergenstock MK and Murphy M: Autophagy in tumor suppression and cancer therapy. *Critical Reviews in Eukaryotic Gene Exp* 21: 71-100, 2011.
31. Lebovitz CB, Bortnik SB and Gorski SM: Here, there be dragons: Charting autophagy-related alterations in human tumors. *Clin Cancer Res* 18: 1214-1226, 2012.
32. BenYounès A, Tajeddine N, Tailler M, Malik SA, Shen S, Métivier D, Kepp O, Vitale I, Maiuri MC and Kroemer G: A fluorescence-microscopic and cytofluorometric system for monitoring the turnover of the autophagic substrate p62/SQSTM1. *Autophagy* 7: 883-891, 2011.
33. Komatsu M, Kurokawa H, Waguri S, Taguchi K, Kobayashi A, Ichimura Y, Sou YS, Ueno I, Sakamoto A, Tong KI, *et al*: The selective autophagy substrate p62 activates the stress responsive transcription factor Nrf2 through inactivation of Keap1. *Nat Cell Biol* 12: 213-223, 2010.
34. Kundu M: ULK1, Mammalian Target of Rapamycin, and Mitochondria: Linking Nutrient Availability and Autophagy. *Antioxid Redox Signal* 14: 1953-1958, 2011.
35. Cheong H and Klionsky DJ: Dual role of Atg1 in regulation of autophagy-specific PAS assembly in *Saccharomyces cerevisiae*. *Autophagy* 4: 724-726, 2008.
36. Luciani MF, Giusti C, Harms B, Oshima Y, Kikuchi H, Kubohara Y and Golstein P: Atg1 allows second-signal autophagic cell death in *Dictyostelium*. *Autophagy* 7: 501-508, 2011.
37. Yorimitsu T, Nair U, Yang Z and Klionsky DJ: Endoplasmic reticulum stress triggers autophagy. *J Biol Chem* 281: 30299-30304, 2006.

38. Tekirdag KA, Korkmaz G, Ozturk DG, Agami R and Gozuacik D: MIR181A regulates starvation- and rapamycin-induced autophagy through targeting of ATG5. *Autophagy* 9: 374-385, 2013.
39. Lopez-Terrada D, Cheung SW, Finegold MJ and Knowles BB: Hep G2 is a hepatoblastoma-derived cell line. *Hum Pathol* 40: 1512-1515, 2009.
40. Kenneth J and Livak TD: Analysis of relative gene expression data using real-time quantitative PCR and the 2(-Delta Delta C(T)) method. *Method* 25: 402-408, 2001.
41. Simasi J, Schubert A, Oelkrug C, Gillissen A and Nieber K: Primary and secondary resistance to tyrosine kinase inhibitors in lung cancer. *Anticancer Res* 34: 2841-2850, 2014.
42. Quintás-Cardama A, Kantarjian HM and Cortes JE: Mechanisms of primary and secondary resistance to imatinib in chronic myeloid leukemia. *Cancer Control* 16: 122-131, 2009.
43. Schleicher SM, Moretti L, Varki V and Lu B: Progress in the unraveling of the endoplasmic reticulum stress/autophagy pathway and cancer: Implications for future therapeutic approaches. *Drug Resist Updat* 13: 79-86, 2010.
44. Li T, Su L, Zhong N, Hao X, Zhong D, Singhal S and Liu X: Salinomycin induces cell death with autophagy through activation of endoplasmic reticulum stress in human cancer cells. *Autophagy* 9: 1057-1068, 2013.
45. Su CC: Tanshinone IIA could inhibit pancreatic cancer BxPC-3 cells through increasing PERK, ATF6, Caspase-12 and CHOP expression to induce apoptosis. *J Biom Sci Eng* 8: 149-159, 2015.
46. Liu H, Nishitoh H, Ichijo H and Kyriakis JM: **Activation of apoptosis signal-regulating kinase 1 (ASK1) by tumor necrosis factor receptor-associated factor 2 requires prior dissociation of the ASK1 inhibitor thioredoxin.** *Mol Cell Biol* 20: 2198-2208, 2000.
47. Nakagawa T and Yuan J: Cross-talk between two cysteine protease families activation of caspase-12 by calpain in apoptosis. *J Cell Biol* 150: 887-894, 2000.
48. Morishima N, Nakanishi K, Takenouchi H, Shibata T and Yasuhiko Y: An Endoplasmic Reticulum Stress-specific Caspase Cascade in Apoptosis cytochrome c-independent activation of caspase-9 by caspase-12. *J Biol Chem* 277: 34287-34294, 2002.
49. Bae JY and Park HH: Purification and characterization of a ubiquitin-like system for autophagosome formation. *J Microbiol Biotechnol* 20: 1647-1652, 2010.
50. Satoo K, Noda NN, Kumeta H, Fujioka Y, Mizushima N, Ohsumi Y and Inagaki F: The structure of Atg4B-LC3 complex reveals the mechanism of LC3 processing and delipidation during autophagy. *EMBO J* 28: 1341-1350, 2009.
51. Tanida I, Minematsuikeguchi N, Ueno T and Kominami E: Lysosomal turnover, but not a cellular level, of endogenous LC3 is a marker for autophagy. *Autophagy* 1: 84-91, 2005.
52. Sailaja GS, Praveen B, Bharathi G, Chetty C, Gogineni VR, Velpula KK, Gondi CS and Rao JS: The secreted protein acidic and rich in cysteine (SPARC) induces endoplasmic reticulum stress leading to autophagy-mediated apoptosis in neuroblastoma. *Int J Oncol* 42: 188-196, 2013.
53. Jiang Q, Li F, Shi K, Wu P, An J, Yang Y and Xu C: Involvement of p38 in signal switching from autophagy to apoptosis via the PERK/eIF2 α /ATF4 axis in selenite-treated NB4 cells. *Cell Death Dis* 5: e1270, 2014.
54. Kamada Y: Prime-numbered Atg proteins act at the primary step in autophagy: Unphosphorylatable Atg13 can induce autophagy without TOR inactivation. *Autophagy* 6: 415-416, 2010.
55. Saito A, Ochiai K, Kondo S, Tsumagari K, Murakami T, Cavener DR and Imaizumi K: Endoplasmic reticulum stress response mediated by the PERK-eIF2(α)-ATF4 pathway is involved in osteoblast differentiation induced by BMP2. *J Biol Chem* 286: 4809-4818, 2011.
56. Kimura S, Noda T and Yoshimori T: **Dynein-dependent movement of autophagosomes mediates efficient encounters with lysosomes.** *Cell Struct Funct* 33: 109-122, 2008.
57. Lee H, Noh JY, Oh Y, Kim Y, Chang JW, Chung CW, Lee ST, Kim M, Ryu H and Jung YK: IRE1 plays an essential role in ER stress-mediated aggregation of mutant huntingtin via the inhibition of autophagy flux. *Hum Mol Genet* 21: 101-114, 2012.
58. Zhang C, Kawauchi J, Adachi MT, Hashimoto Y, Oshiro S, Aso T and Kitajima S: Activation of JNK and Transcriptional Repressor ATF3/LRF1 through the IRE1/TRAF2 pathway is implicated in human vascular endothelial cell death by homocysteine. *Biochem Biophys Res Commun* 289: 718-724, 2001.
59. Shvets E, Fass E, Scherz-Shouval R and Elazar Z: The N-terminus and Phe52 residue of LC3 recruit p62/SQSTM1 into autophagosomes. *J Cell Sci* 121: 2685-2695, 2008.
60. Liu WJ, Ye L, Huang WF, Guo LJ, Xu ZG, Wu HL, Yang C and Liu HF: p62 links the autophagy pathway and the ubiquitin-proteasome system upon ubiquitinated protein degradation. *Cell Mol Biol Lett* 21: 29, 2016.



This work is licensed under a Creative Commons Attribution-NonCommercial-NoDerivatives 4.0 International (CC BY-NC-ND 4.0) License.